Frontiers in Mechanochemistry and Mechanical Alloying

INCOME2008
1-4 December, 2008

SYNTHESIS OF NANOCRYSTALLINE AND AMORPHOUS PHASES IN COMPLEX METALLIC ALLOYS DURING MECHANICAL MILLING

N.K. Mukhopadhyay [ξ]
Centre of Advanced Study, Department of Metallurgical Engineering
Institute of Technology, Banaras Hindu University
Varanasi-221005, India

Keywords: Complex metallic alloys, Intermetallics, Amorphous phase, Disordering, Nanocrystals, Mechanical milling, Nanocrystals

Abstract

The synthesis of nanocrystalline, amorphous and their composite phases in complex metallic alloys (CMAs) appears to be beneficial in order to overcome the brittleness problem of these alloys. Mechanical milling among the various processing techniques, have been adopted for the purpose of synthesizing nano-phase/amorphous and their composites. The aim of the present work is to investigate the stability and phase evolution on some complex metallic alloys during mechanical milling. The milling is carried out in a planetary ball mill at various milling intensity with varying the ball to powder ratio in a suitable milling medium. The samples are characterized with the help of XRD, SEM and TEM. It is found that these alloys can give rise to the formation of nanocrystalline phases of grain sizes to a certain minimum value as well as amorphous phase. At present it is not clear why, given a milling energy, some alloy systems restrict to the formation of nanograin of a particular size and do not lead to the complete formation of amorphous phase. Attempts will be made to discuss the evolution and stability of these nano/ amorphous phases based on the modified Miedema model of free energy by including the contribution from grain size effects generated during milling.

Introduction

It is known that non-equilibrium processing techniques can be exploited to raise the free energy of a system and then to allow it by relaxing to a stable/ metastable phase. The properties of the metastable phases can be beneficial in many respects. There are intense activities to understand the origin and role of complex intermetallic phases for developing advanced materials while experimenting with the various non-equilibrium processing techniques [1-3]**.** The aim of the non-equilibrium processing techniques can be illustrated in Fig.1. It shows that by changing the temperature and pressure the system can be raised to a level far from the equilibrium and then allowed to attain the stable/ metastable configuration [4]. There are several non-equilibrium techniques that have been developed during the past few decades to synthesize novel materials. These include rapid solidification processing, mechanical alloying/milling, plasma processing, vapor deposition, ion or electron or neutron irradiation [1-5]. Among all these techniques mechanical alloying/ milling, a solid state powder processing technique appears to be an ideal processing route to develop nanocrystalline materials at an ambient temperature. It has been demonstrated that by changing the milling intensity it is possible to obtain crystalline, quasicrystalline, amorphous and composites phases in Al-Cu-Mn alloys (Fig. 2) [4]. Mechanical alloying/milling can convert an intermetallic compound including quasicrystals or elemental powder blend into nanocrystalline or amorphous aggregate in addition to the metastable phases depending on the milling parameters [1-7]. One of the advantages of this conversion to nanocrystalline or amorphous state is the enhancement of ductility and toughness in the brittle intermetallics. Recently there is a renewed interest to investigate the complex metallic alloys (CMAs) from structural and application point of view [8]. The complex metallic alloys are understood to be those alloys which possess a complex crystal structure unlike simple crystalline system. The clusters of atoms are present in the unit cell. In addition, quasicrystalline materials which do not possess periodicity can also be classified under complex metallic alloys. There are close similarities among the quasicrystals and several complex intermetallics. In fact bulk metallic glasses, a new class of materials which are so complex in the form of compositions and elemental combination can be categorized under CMAs. It may also possible to realize the high entropic alloys which consist of multi-component and equiatomic elements are close to the compositionally complex bulk metallic glasses.

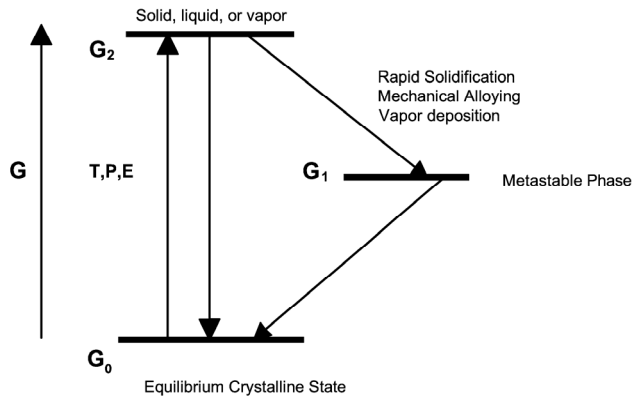

Figure 1. Schematic diagram of free energy of the system during nonequilibrium processing [3]

[ξ] email: mukho_nk@rediffmail.com

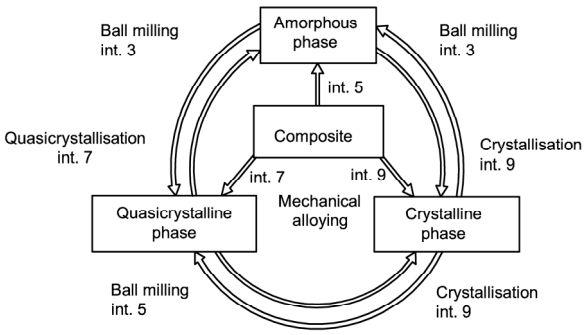

Figure 2. Schematic diagram to show the transformation among various phases during mechanical milling/alloying in Al-Cu-Mn alloys [4]

The challenging task in this field is to enhance the ductility or toughness of these CMAs by way of modifying the microstructures and or crystals structure. It appears that during mechanical alloying/milling of CMAs, the accumulation of deformation generated defects including significant increase in internal surface area (grain boundaries) could lead to the formation of ductile or tougher materials by converting crystalline/quasicrystalline phases into nanocrystalline/nanoquasi-crystalline/amorphous phases or their composites [6,9,10]. Therefore, it is interesting to study the free energy of the phases and their relative stability in course of milling.

In the present investigation, γ-brass intermetallic phase in Cu base and Al base alloys, being a complex Hume-Rothery phase have been selected for studying its stability during mechanical milling. The structure of γ-brass alloy is described in terms of a cubic unit cell consisting of 27 cubic units in a 3 x 3 x 3 array of a body centred cubic (bcc) lattice such that the unit cell of γ-brass contains 52 sites with two atoms - one at the centre and another at the vertices of this block - being removed [11]. The same structure is also described in terms of a cluster of four concentric shells centered on the vacant sites (Fig. 3) [12,13].

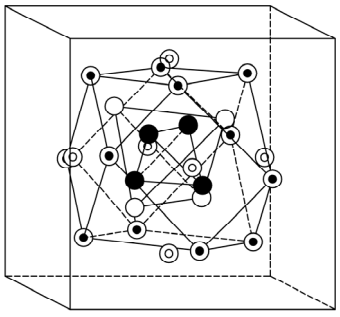

Figure 3. The schematic diagram of a typical cluster present in γ-brass structure [9]

As shown in Fig. 3, the first shell, a regular tetrahedron of four atoms is surrounded by the second comprising four more atoms and forms a larger tetrahedron. The third shell is an octahedron containing six atoms. The fourth one is cuboctahedron containing twelve atoms. Thus γ-brass is a bcc structure with a cluster of 26 atoms occupying the body centre and vertex position of the cubic unit cell [14]. The Al_4Cu_9 γ-brass structure is a simple cubic structure unlike γ-Cu_5Zn_8 which is a bcc structure. In addition to the bcc γ-brass alloy and simple cubic (sc), face centered cubic (fcc) γ-brass structure has also been reported in Al-Cu based alloys. The crystal structure of γ-brass phase is fairly well understood in terms of cluster compound. However, the stability of these clusters and the scope of synthesis of nanocrystalline or amorphous state by mechanical milling have not yet been explored.

The aim of the present investigation is to review our understanding and to study further the phase transformation of γ – brass in Cu-Zn binary and Al based ternary systems (Al-Cu-Cr, Al-Cu-Fe and Al-Cr-Fe) during mechanical milling and their relative stability. The attempts have been made to compute the free energy by using a semi-empirical Miedema model in order to compare their stability and the possibility of synthesizing nanocrystalline or amorphous aggregate during mechanical alloying/milling. The basis for free energy calculation using the Miedema model has been discussed in the subsequent section.

Thermodynamic Analyses

Thermodynamic approach has been adopted to predict the composition range and degree of grain refinement necessary to initiate solid state amorphization through mechanical milling by calculating the Gibbs free energy changes as a function of composition and crystallite size using appropriate modification of the Miedema model [16,17]. It is illustrative, though not strictly rigorous, to calculate and compare approximate Gibbs free energies of the formation for the anticipated phases during mechanical milling of the present alloys.

Following Miedema semi-empirical theory [18], the Gibbs free energy of solid solution (ss) can be evaluated as:

$$\Delta G_{ss} = \Delta H_{ss} - T\,\Delta S_{ss} \quad (1)$$

It can be pointed out that in micron grain size materials the effect of grain size or crystallite size has negligible contribution to the free energy, whereas in case of nanomaterials, the grain size will have a significant effect on the free energy of crystalline state. In addition to the interfacial energy, the strain energy has also an effect. However, in the present calculation we are ignoring the effect due to strain energy, which will be dealt with elsewhere. Now the equation (1) can be modified as:

$$\Delta G_{crys} = \Delta G_{ss} + \Delta G_{\gamma} \quad (2)$$

where, ΔH_{ss} and ΔS_{ss} are the enthalpy and entropy of mixing, respectively where as ΔG_{γ} term refers to interfacial contributions and $\Delta G_{\gamma} = 4\gamma\, V_m/d_c$, where d_c represents average grain size and γ is the interfacial energy [19-20]. This approach has been extended to ternary alloy [21]. The following calculation has been shown based on ternary alloys from which the binary one can be easily deduced. We shall use the entropy of mixing for an ideal solution:

$$\Delta S_{ss} = -R\,(X_A \ln X_A + X_B \ln X_B + X_C \ln X_C) \quad (3)$$

where, X_A, X_B and X_c are the mole fraction of elements A, B and C, and R is the gas constant.

The enthalpy of formation of a solid solution can be written as [18, 22]:

$$\Delta H_{ss.}^{ABC} = \Delta H_c^{ABC} + \Delta H_e^{ABC} + \Delta H_s^{ABC} \quad (4)$$

where, ΔH_c, ΔH_e and ΔH_s are the chemical, elastic and structural contributions due to mixing of the different atoms, the atom size mismatch and taking into account the difference in valence and crystal structure of solute and solvent respectively. Compared with the first two terms, the structural contributions have only a minor effect [23], which will be ignored here. Thus for a ternary system:

$$\Delta H_{ss}^{ABC} = \Delta H_c^{ABC} + \Delta H_e^{ABC} \quad (5)$$

where,

$$\Delta H_c^{ABC} = \Delta H_c^{AB} + \Delta H_c^{BC} + \Delta H_c^{AC} \quad (6)$$

From the Miedema and Niessen model [17,21]:

$$\Delta H_c^{AB} = X_A X_B (f_B^A \Delta H_{sol}^{A \text{ in } B} + f_A^B \Delta H_{sol}^{B \text{ in } A}) \quad (7)$$

where, $\Delta H_{sol}^{A \text{ in } B}$ is the solution enthalpy of A in B:

$$\Delta H_{sol}^{A \text{ in } B} = [V_A^{2/3} / (n_{ws}^{-1/3})_{av}] [- p (\Delta \Phi)^2 + Q (\Delta n_{ws}^{1/3})^2] \quad (8)$$

$$f_B^A = C_B [1 + k(C_A C_B)^2] \quad (9)$$

$$C_B = X_B V_B^{2/3} / (X_B V_B^{2/3} + X_A V_A^{2/3}) \quad (10)$$

where, V, Φ and n_{ws} are molar volume, work function and electron density of the constituents. f_B^A is the degree by which A atom is surrounded by B atoms and C is the surface concentration of atom. P and Q are empirical constants having the same value for widely different metal combinations. Where, k is taken to be 5 for short-range order (amorphous) and 8 for long-range order, respectively.

$$\Delta H_e^{ABC} = \Delta H_e^{AB} + \Delta H_e^{BC} + \Delta H_e^{AC} \quad (11)$$

$$\Delta H_e^{AB} = X_A X_B (f_B^A \Delta E_e^{A \text{ in } B} + f_A^B \Delta E_e^{B \text{ in } A}) \quad (12)$$

where, $\Delta E_e^{A \text{ in } B}$ is the size mismatch contribution to the enthalpy of solution of A in B per mol A, which can be estimated [24]:

$$\Delta E_e^{A \text{ in } B} = \{2 K_A \mu_B (V_B - V_A)^2\} / \{3 K_A V_B + 4 \mu_B V_A\} \quad (13)$$

where, K and μ are bulk modulus and shear modulus respectively. The Enthalpy of formation of the amorphous phase for ternary system can be estimated from:

$$\Delta H \text{ (amorphous)} = \Delta H_c + 3.5 (X_A T_{m,A} + X_B T_{m,A} + X_C T_{m,C}) \quad (14)$$

But for ternary system, Gibbs free energy of formation of the amorphous phase can be estimated from [25]:

$$\Delta G_a = \Delta H_a - T\Delta S_a + X_A \Delta G_A^{a-c}(T) + X_B \Delta G_B^{a-c}(T) + X_c \Delta G_c^{a-c}(T) \quad (15)$$

where, ΔH_a and ΔS_a are the enthalpy and entropy of mixing of the amorphous phase. $\Delta G^{a-c}(T)$ is the difference in Gibbs free energy between the amorphous and crystalline phases of the pure element at the room temperature. ΔH_a contains only the chemical contribution due to the amorphous structure, which can be calculated from Eq. (6) using a value of 5 for the constant k. ΔS_a can be calculated from Eq. (3). Because the MA device was water-cooled, we can assume that the temperature of MA was at room temperature. $\Delta G^{a-c}(T)$ can be estimated from:

$$\Delta G^{a-c}(T) = K_{corr} \Delta H_f (T_m - T) / T_m \quad (16)$$

where, ΔH_f and T_m are enthalpy of fusion and melting temperature respectively and K_{corr} is the correction coefficient, the value of which can be taken as [26]:

$$K_{corr} = 7 T / (6T + T_m) \quad (17)$$

Thus following the above formalism, the free energy of various phases in binary and ternary alloys has been calculated.

Experimental

γ-brass alloys in Cu based and Al-based systems (Al-Cu-Cr, Al-Cu-Fe, Al-Cr-Fe) phases were prepared by induction melting using commercially pure elements. Following homogenization the ingot being highly brittle was easily crushed to powder of less than 0.1 mm size. High-energy ball milling was carried out in a P5-planetary/ Retsch mill, at various milling intensities. Milling was continued up to a maximum milling time of 50 h. The milling has been carried out in wet condition using toluene as medium to prevent oxidation, agglomeration and welding to milling devices during milling. The milling parameters were adjusted in such a way so that the contamination during milling can be negligible. The contamination was checked by chemical analysis and x-ray diffraction techniques. The composition of as-cast alloy was determined by energy dispersive x-ray spectroscopy (EDX) attached to the SEM using a JEOL 840A model operating at 15 kV. The identity and sequence of phase evolution in different stages of mechanical milling were studied by X-ray diffraction (XRD) analysis using a Rigaku diffractometer with Cu-K_α and Co-K_α radiation. The average crystallite size was determined from broadening of the most intense peak of the concerned phases after the elimination of the contributions due to instrumental and strain effects. The results of the XRD analysis concerning grain size and amorphization were confirmed by transmission electron microscopy using a JEOL 2100F model operating at 200 kV.

Results and Discussion

Figure 4 shows XRD patterns of the as-cast alloy as well as milled alloys revealing the presence of a single phase γ-Cu_5Zn_8. The crystal structure was found out to be a complex bcc with a lattice parameter of 0.88 nm. The structural changes as analyzed from the XRD analysis in course of mechanical milling (milled with BPR 15:1) can be realized from the Fig. 4. No new phases including amorphous structure can be identified even after 40 h of milling. Instead, the XRD peaks undergo further broadening due to grain refinement and accumulation of lattice strain. Milling was also carried out with BPR 30:1 upto 40 h. However, increasing the milling intensity with a higher BPR did not lead to evolution of any new phases. There is a continuous reduction in the average crystallite size during different stages of mechanical milling from 10 to 40 h. The crystallite size varied from an average of 45 nm to 30 nm with BPR 15:1, 30 nm to 25 nm by milling with BPR 30:1

(Fig. 5(a)) and 40 nm to 30 nm by alloying with BPR 15:1. The average strain induced increased continually during various stages of mechanical milling and alloying from 10 to 40 h. The strain induced varied from an average 0.44 % to 0.47 % with BPR 15:1, 0.45 % to 0.51 % with BPR 30:1 by milling (Fig. 5(b)) and 0.43 % to 0.48 % with BPR 15:1 by mechanical alloying.

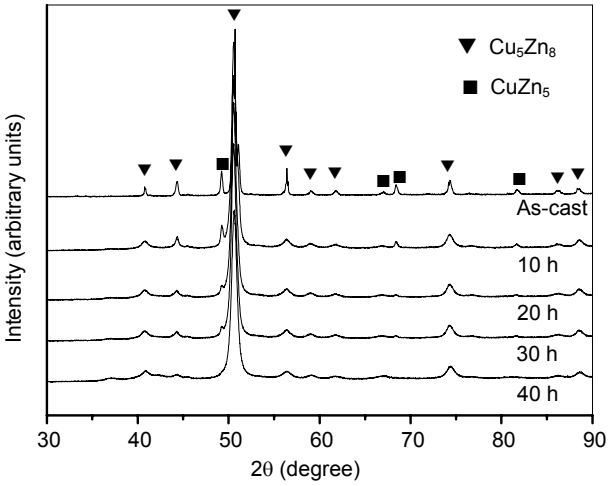

Figure 4. XRD pattern of mechanically milled as-cast Cu_5Zn_8 alloy having BPR 15:1 using λ = 1.789 Å for 10 h, 20 h, 30 h and 40 h

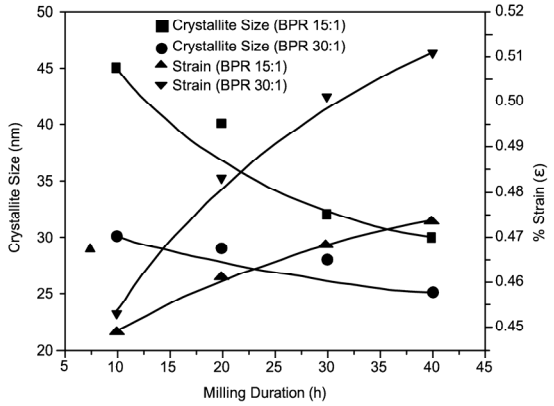

Figure 5. Variation of crystallite size and strain with milling duration with BPR 15:1 and 30:1

TEM analysis of the 40 h milled with a BPR of 30:1 was done which shows the rings corresponding to the γ-brass phase (Fig. 6(a)). The 'd' values obtained after indexing of the ring pattern were compared with that obtained by X-ray analysis. The two sets of values match with each other, which confirms the presence of γ-phase in the 40 h milled sample. The powder particle size for the 40 h milled (BPR 30:1) powder of γ-brass alloy is found to be about 0.1 μm (Fig. 6(b). The bright field and dark field images show the presence of nano domains with an average crystallite size of about 20 nm (Fig. 6(c) & (d)). The free energy of different products (solid solution, amorphous and intermetallic) in a binary system can be calculated using the Miedema model as discussed earlier. The contribution of grain boundary energy has been incorporated in the free energy expression.

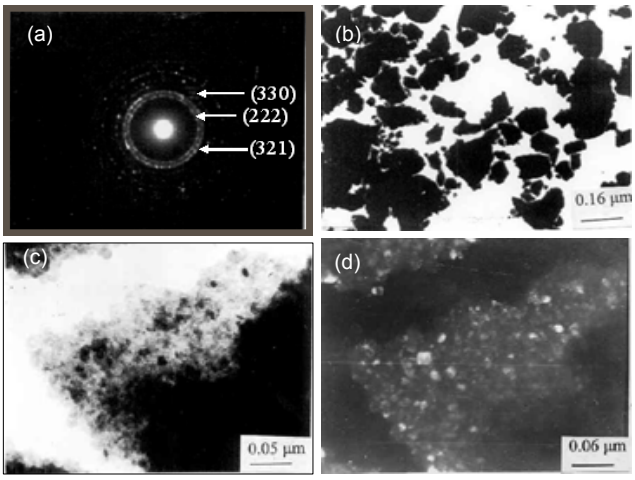

Figure 6. (a) Selective area electron diffraction pattern of 40 h milled sample (BPR 30:1) of the Cu-Zn γ-brass alloy. TEM photomicrographs showing (b) Particle size after 40 h of milling, (c) Bright field image of the nano γ-phase & (d) Dark field image corresponding to the nano γ-phase ring

Figure 7 shows the variation of ΔG (for amorphous, three intermetallic compounds and crystalline solid solutions) as a function of composition for different values of d_c of the crystalline intermetallic compounds and solid solution phase and hence different levels of ΔG_γ contributions for the binary system Cu-Zn. It is evident that crystalline solid solution (of large crystallite size where ΔG_γ can be neglected) is more stable than its amorphous counterpart in the entire composition range and particularly the intermetallics are most stable phases in terms of Gibbs free energy values. It is apparent that amorphization is possible below 50 nm if the Cu-Zn alloy is in solid solution state prior to milling. The solid solution ranging from 27.7 to 69.2 at. % Cu is possible to amorphize corresponds to d_c below 25 nm. Further reduction in grain size increases ΔG. The intermetallic phases (Cu-Zn, γ-Cu_5Zn_8, $CuZn_5$), are the most stable phases and difficult to amorphize. Only $CuZn_5$ phase can transform to amorphous phase at $d_c < 10$ nm, and to convert the other two phases (γ-Cu_5Zn_8, Cu-Zn) into amorphous state the phase grain size should be below 8 nm. The above discussion supports the results obtained from XRD and TEM analysis of the milled powder where XRD data suggests that the phases are intermetallic prior to and after milling. Grain size of γ-Cu_5Zn_8 could not be reduced below 25 nm even after 30/40 h of milling operation. It is obvious from the experimental data that grain size reduction has reached nearly steady state size and the reduction of the crystallites beyond that size will be difficult. Therefore it will be difficult to reduce the grain size further below ~ 20 nm as prolonged milling will cause heating, contamination and loss of Zn. The heating effect will prevent further reduction as the diffusivity at this milling temperature will be high enough to restore the original crystallite size. This is due to the fact that the diffusivity at this temperature in nanoscale microstructure is expected to be high. In fact this is similar to the situation why in case of low melting point material the attainment of nano grain sizes are difficult compared to that of high melting point material [1].

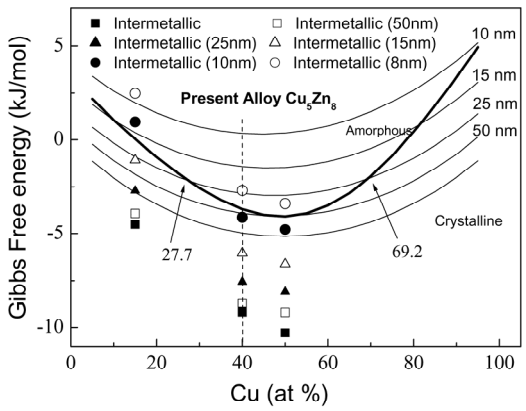

Figure 7. Gibbs free energy of the amorphous, solid solution and intermetallic (Cu-Zn, γ-Cu_5Zn_8, $CuZn_5$) phases of Cu-Zn systems as a function of composition and grain size

We have also investigated the Al-based γ- $(Cu_9Al_4)_{94.5}Cr_{5.5}$ phase which is sc gamma brass phase (cP52) reported in Al-Cu alloys. Figure 8 reveals the XRD patterns obtained from the γ-($Al_4Cu_9)_{94.5}Cr_{5.5}$ samples subjected to mechanical milling (BPR 15:1) for different ranges of milling time in a Retsch PM 400 planetary ball mill. The low intensity peaks are all present at the initial stage (1 h) but soon undergo mutual dissolution after 10 h of milling. The 50 h milled powder of γ- $(Al_4Cu_9)_{94.5}Cr_{5.5}$ alloy did not reveal any significant phase transition or new phase formation but it led to the formation of disordered phase which resembles bcc γ-brass structure as the (300) peak disappeared completely. In addition, some amount of amorphous phase overlapping with the broadened (330) peak of nanocrysalline phases, can be expected to co-exist with the nanocrystalline phases and this has been further confirmed during TEM/HREM investigation. Continued ball milling up to 50 h yields the same single-phase product with a crystallite size 20 nm. The crystallite size varied from 45 nm to 20 nm during different stages of milling from 10 to 50 h whereas strain induced varied from 0.60 % to 0.99 % during various stages of milling from 10 to 50 h.

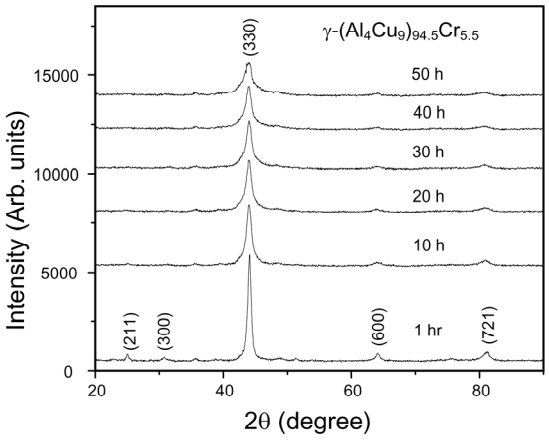

Figure 8. XRD Patterns of mechanically milled as-cast γ-($Al_4Cu_9)_{94.5}Cr_{5.5}$ alloy for 1 h, 10 h, 20 h, 30 h, 40 h and 50 h with BPR 15:1

It has been analyzed from the SAD pattern that powder particle at this stage consists of disordered nanocrystalline single phase material with an average lattice parameter of 0.872 nm (Fig. 9). Figure 10 shows the high resolution TEM image of the 50 h milled powder. The microstructure is predominantly nanocrystalline with grain sizes in the range of 20-40 nm. It is interesting to note that the regions between the nanocrystalline grains seem to contain amorphous regions. The EDX analysis also confirms the same composition of the amorphous and nanocrystalline phase. It indicates that the further milling will give rise to complete amorphization**.** It can be mentioned that the amount of amorphous phase by HREM technique has been overestimated.

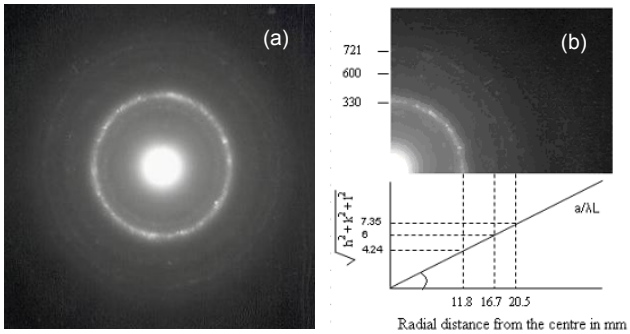

Figure 9. SAD pattern of the 50 h milled powder of γ-($Al_4Cu_9)_{94.5}Cr_{5.5}$ alloy showing a number of diffuse rings with several diffraction spots coinciding with the rings

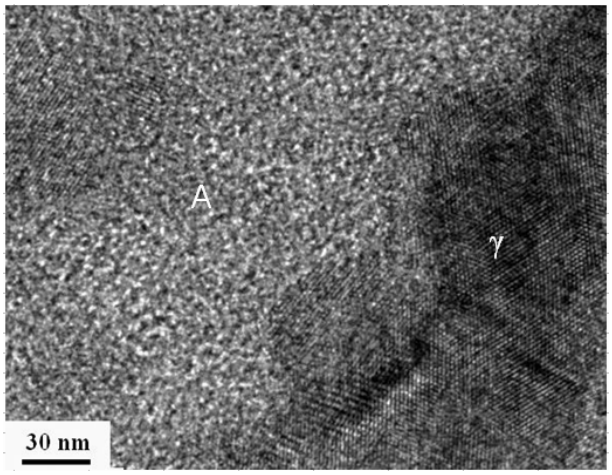

Figure 10. A high resolution TEM image of 50 h milled product of the γ-($Al_4Cu_9)_{94.5}Cr_{5.5}$ alloy showing a predominantly nano-crystalline microstructure (γ) with some amorphous regions (A)

The results obtained from these calculations for Al-Cr-Cu system maintaining the stoichiometric ratio $(Cu_9Al_4)_{(1-x)}Cr_x$ have been plotted as ΔG-x (Gibbs energy versus composition) diagram for different values of d_c of the crystalline solid solution phase and hence different levels of ΔG_γ contributions as shown in Fig. 11. It is evident that a crystalline solid solution is more stable than its amorphous counterpart in the entire composition range. Therefore,

it is clear from the diagrams that the formation of amorphous phase for this system is not thermodynamically possible under equilibrium condition as solid solution (polycrystalline) is more stable than the amorphous phase. However amorphization seems possible for this alloy when the grain size decreases below 25 nm during milling. The solid solution ranging from 0 to 0.54 mole fraction Cr is possible to amorphize with a corresponding d_c below 20 nm. Further reduction in grain size increases ΔG of the system such that curve (for d_c = 15 nm) is way above the curve for amorphous phase up to 0.68 mole fraction Cr. So high energy ball milling for longer period of time may give rise to amorphous phase in this range as the particle size decreases with milling time.

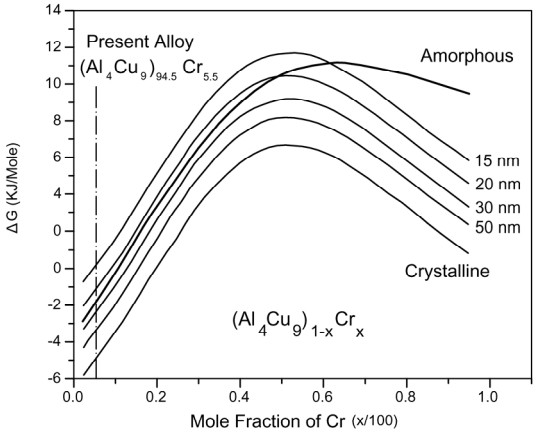

Figure 11. Gibbs free energy-composition plot of the amorphous and crystalline solid solution for Al-Cr-Cu system maintaining the stoichiometric ratio $(Al_4Cu_9)_{(1-x)}Cr_x$ as a function of composition and grain size

The above discussion supports the results obtained from TEM and HRTEM analysis of 50 h milled powder of γ-($Al_4Cu_9)_{94.5}Cr_{5.5}$ alloy which shows the formation of amorphous phase along with the nanocrystalline phases having grain size in the range of 20 to 40 nm. A similar type of trend in terms of nanocrystallization and amorphization has been observed in case of the HRTEM images and free energy plots from Al-Cu-Fe (Fig. 12 and 13) and Al-Cr-Fe (Fig. 14 and 15) γ brass alloys. The concerned free energy plot also exhibits the crossover of the crystalline and amorphous phases. However it can be realized that in case of the Al-Cr-Fe γ brass alloys, the amorphization was much more prominent compared to the other alloys. This effect can be attributed to the fact that Al-Cr-Fe is of high melting and Cu-Zn is of low melting alloys. Hence to stabilize the amorphous phase it is necessary to reduce the grain size below a limit. In many cases, this limit to attain will not be easy if not impossible because of the recovery and recrystallization effects. Hence the amorphization cannot be achieved in such alloys even though the crystal structure could belong to CMAs. It can be seen from the trend of the plot that the rate of reduction of the grain size and strain effect has reached a steady state condition at higher BPR. Therefore the significant grain refinement is not expected during further course of milling and the strain will not enhance as the dislocation mechanics will not play any further role during milling. Only fracturing and grain rotation are expected to accommodate the stress arising from the milling. Hence it will be interesting to study further the effect of the melting temperature on the minimum grain sizes attained during milling and the amorphizability.

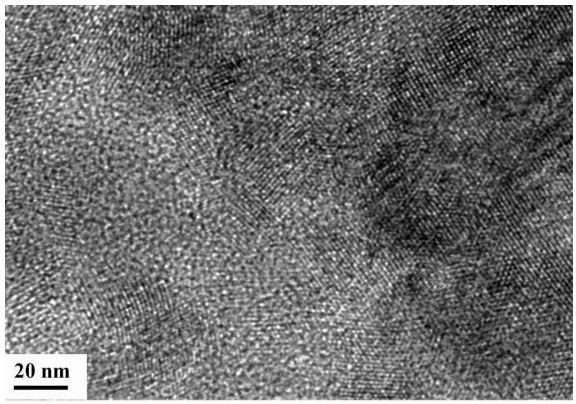

Figure 12: A high resolution TEM image of 50 h milled product of the γ-(AlCuFe) alloy showing a predominantly nanocrystalline microstructure (γ) with some amorphous regions (A)

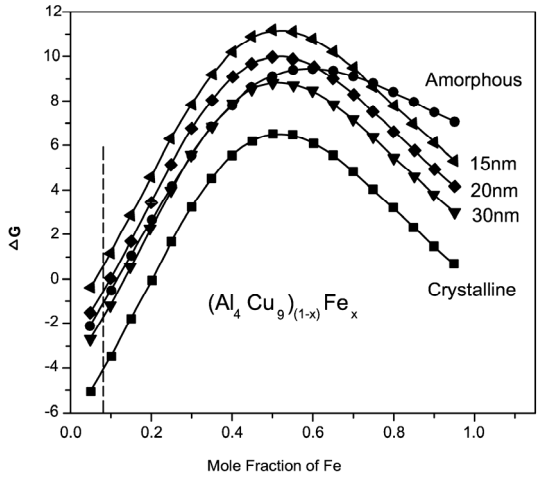

Figure 13: Gibbs free energy-composition plot of the amorphous and crystalline solid solution for Al-Fe-Cu system as a function of composition and grain size.

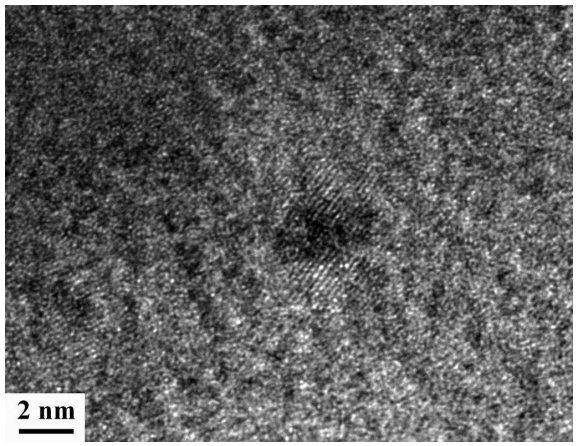

Figure 14: A high resolution TEM image of 50 h milled product of the γ-(AlCuFe) alloy showing a predominantly nanocrystalline microstructure (γ) with some amorphous regions (A)

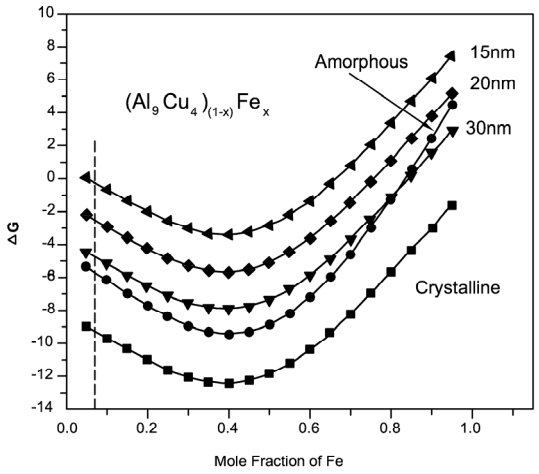

Figure 15: Gibbs free energy-composition plot of the amorphous and crystalline solid solution for γ-(AlCrFe) system as a function of composition and grain size

Concluding Remarks

Single phase γ-brass phase in Cu-Zn and Al-based system (Al-Cu-Cr, Al-Cu-Fe, Al-Cr-Fe) has been milled under various milling parameters. Milling of Cu-Zn γ-brass has led to the nanocrystallization without formation of amorphous or any other metastable phases. Whereas, milling of Al-Cu-Cr, Al-Cu-Fe and Al-Fe-Cr γ-brass alloys gives rise to the formation of nanocrystalline phase with 15-30 nm size along with amorphous phase, the amount of which varies in these three different alloys. The degree of amorphization was found to be significant in Al-Fe-Cr alloys which can be attributed to higher homologous temperature. The reduction of grain sizes below a certain level appears to be difficult and it is dependent on the system. It can also be understood that in case of low melting intermetallic alloys, the heating effect during milling can cause easy recovery and high diffusivity during milling, which subsequently can lead to recovery and recrystallization rather than reduction of grain sizes. As a result the grain size and the induced lattice strain reach the steady state condition. Thermodynamic analyses using modified Miedema model lends support to explain the experimental results in terms of amorphization and nanocrystallization of the milled materials. It can be mentioned that the Gibbs free energy of the system after taking care of interfacial contribution due to grain refinement suggest that below a certain grain size, amorphous phase will be stable over nanocrystalline phase and the amorphization will occur easily. However it is not clear why crystalline phases in the form of nanocrystals are present along with the amorphous phase.

Acknowledgements

The author would like to thank Profs D.H. Kim, I. Manna and B.S. Murty for fruitful collaboration through out the years. The author would also like to acknowledge the contribution in terms of experimental work and discussion with the students - Mr T.P Yadav, Mr R. Manna, D. Mukherjee and S. Dutta. The financial support of the Department of Science and Technology (DST Project: SR/S3/ME/051/2005-SERC-Engg), New Delhi, India for carrying out this work is gratefully acknowledged.

References

1. B.S. Murty, S. Ranganathan, *Int. Mater. Rev*., 43 (1998) 101.
2. N.K. Mukhopadhyay, J. Bhatt, A.K Pramanick, B.S Murthy, P.Paufler, *Journal of Material Science,* 39 (2004) 5155.
3. C. Suryanarayana, *Progress in Material Science,* 46 (2001) 1.
4. J. Eckert, L. Schultz, K. Urban, *Appl. Phys. Lett*., 55 (1989) 117.
5. I. Manna, P. Nandi, B. Bandyopadhyay, K. Ghoshray, A. Ghoshray, *Acta Materialia,* 52 (2004) 4133.
6. G. Zhou, H. Bakker, *Materials Science and Engineering*, A179/A180 (1994) 453.
7. N.K Mukhopadhyay, T.P Yadav, O.N. Srivastava, *Philosophical Magazine Letters*, 83 (2003) 423.
8. N. K. Mukhopadhyay, *Current Science*, 89 (2005) 1655.
9. N.K Mukhopadhyay, D. Mukherjee, S. Dutta, R. Manna, D.H. Kim, I. Manna, *J. Alloys and Compounds*, 457 (2008) 177.
10. H. Baker, G.F. Zou, H. Yang, *Prog. Mater. Sci.,* 39 (1995) 189.
11. A.J. Bradley, J. Thewlis. *Proc. Roy. Soc.,* A112 (1928) 678.
12. A.J. Bradley, P. Jones, *J. Inst. Met.,* 51 (1933) 131.
13. L. Arnberg, *Chem. Commun.* No. 2. (1979) 1.
14. N.K. Mukhopadhyay, D.Mukherjee, S. Bera, I. Manna, R. Manna, *Materials Sci. Engg.A,* 485 (2008)673
15. N.B. Pearson, J.K. Brandon, R.Y. Brizard, *Z. Kristallogr.*, 143 (1976) 387.
16. A.K. Niessen, P.R. de Boer, R. Boom, P.F. de Chiitel, W.C.M. Mattene, A.R. Miedema, *CALPHAD,* 7 (1983) 51.
17. A.R. Miedema, P.F. de Chatel, F.R. de Boer, *Physica*, 100B (1980) 1-28.
18. A.K. Niessen, A.R. Miedema, *Physica,* 151B (1988) 401.
19. R.B. Schwarz, C.C. Koch, *Appl. Phys. Lett.*, 49 (1986) 146.
20. L.E. Murr, *Interfacial Phenomena in Metals and Alloys,* Addison-Wesley Pu Publishing Company, (1975).
21. L.J. Gallego, J.A. Somoza, J.A. Alonso, *J. Phys. Cond. Matte.,* 2 (1990) 6245.
22. A.R. Miedema, F.R. De Boer,R Boom, *Physica,* 103B (1981) 67.
23. J.M. López, J.A. Alonso, L.J. Gallego, *Phys. Rev.* B36 (1987) 3716-3722.
24. A.K. Niessen, A.R. Miedema, Ber. Bunsenges, *Phys. Chem.,* 87 (1983) 717-723.
25. L.J. Gallego, J.A. Somoza, J.A. Alonso, J.M. López, *J. Phys. F, Met. Phys.,* 18 (1987) 2149.
26. H.B. Singh, A. Holz, *Solid State Commun*., 45 (1983) 985.